Shape and Position of Middle-Angle Scattering Peaks from Smectic Phases of Polymers

N. STRIBECK, C. WUTZ

Universität Hamburg, Institut für Technische und Makromolekulare Chemie, 20146 Hamburg, Germany

Received 17 June 1999; revised 6 May 2001; accepted 10 May 2001

ABSTRACT: A method for the quantitative analysis of isotropic middle-angle X-ray scattering (MAXS) from segmented polymers, which are able to form liquid-crystalline (LC) phases, is proposed and applied to scattering curves from poly(ester imide) samples. Oriented material in the LC state shows MAXS fiber patterns with a meridional layer-line reflection, which sometimes is split, creating a four-point pattern. Comparing scattering data from oriented material with data from isotropic material, we can explain the asymmetry of the isotropic MAXS reflection by limited lateral correlation. Thus, for the LC state of segmented polymers, the notion of stacks built from alternating planar layers of smectic mesogens and spacers units is not generally applicable. Only in the limiting case of infinite flatness does the line profile become symmetric. A simple analytical expression for the shape of the line profile of MAXS reflections is deduced. The equation fitted to the MAXS peak of isotropic LC polymer samples in the smectic state results not only in the determination of a corrected long period but also in two additional parameters, the correlation height of the smectic stack and the flatness of its layers. Compared to established methods for line-profile analysis in small-angle scattering, the proposed method models the nanostructure with classical notions of a two-phase system in one direction only, whereas the lateral contribution to the scattering intensity is characterized by a short-range loss of correlation instead of a classical description by domain-phase boundaries. J Polym Sci Part B: Polym Phys 39: 1749–1755, 2001

Keywords: smectic layers; main-chain liquid-crystalline (LC) polymers; small-angle X-ray scattering; asymmetric reflection; line-shape analysis

INTRODUCTION

Investigating multiblock copolymers that form smectic layer structures with X-ray scattering methods, one generally observes a strong reflection at scattering angles somewhere between the classical small-angle X-ray scattering (SAXS) and wide-angle X-ray scattering (WAXS). Frequently, this reflection is named middle-angle reflection or middle-angle X-ray scattering (MAXS). It originates from a structure formed by alternating layers from mesogens and spacer units along the main chain of the polymer. This peak generally exhibits considerable asymmetry, the origin of which becomes clear when two-dimensional (2D) patterns recorded from drawn fiber material are at hand. Here, instead of point shape or arc shape, one often observes a line-shaped intensity bar, which may degenerate toward a four-point pattern during thermal treatment. From this finding, it follows that the determination of the layer repeat by application of Bragg's law to the peak position in the isotropic scattering curve may lead to significant systematic error. A model for the line shape is to be found that, on the one

Correspondence to: N. Stribeck (E-mail: norbert.stribeck@desy.de)

Journal of Polymer Science: Part B: Polymer Physics, Vol. 39, 1749–1755 (2001)

hand, is adapted to fit the asymmetric profile of the observed peaks and, on the other hand, is simple enough to deal with the broad and unstructured reflections of the distorted structure without the need to introduce many parameters. The 2D data from oriented material indicate a route toward such a model. The predominant effect skewing the MAXS peak is the lateral extension of the layer line, which has to be considered in a model for one-dimensional (1D) data. The aim of this work is the presentation of a corresponding method used to evaluate scattering data of poly(ester imide) (PEI) polymers synthesized by the group of Kricheldorf.[1,2]

Although for nematic structures of stiff-chain polymers considerable fundamental work on the adapted theories and structural analysis of WAXS has been published by the groups of Blackwell[3–7] and Windle,[8–11] for smectic structures there is little work that accounts for their basic features of restricted order.

Smectic phases are observed with polymers containing flexible spacers and rigid mesogens. Mensinger et al.[12] investigated branched polymers with mesogens both in the main chain and in side chains. Isotropic scattering curves and fiber diagrams were studied as a function of temperature concerning peak position and integral intensity. In the fiber diagrams, the azimuthal width of arc-shaped meridional MAXS peaks were discussed in terms of an orientation distribution of lamellar stacks. Francescangeli et al.[13] investigated a main-chain liquid-crystalline (LC) polymer and interpreted the observed layer-line reflection. They made out faint lateral extensions of smectic planes and called the structure "cybotactic nematic". When studying isotropic poly(ester amide) material, Murthy and Aharoni[14] observed MAXS lines of an asymmetrical shape, computed a long period from the position of the intensity maximum, and compared the value to the length of the repeat, known from the chemical structure of the chain. They found that the long period was shorter than the unit repeat. Pardey et al.[15] studied a series of PEI materials. Long periods from MAXS lines with an asymmetrical shape were computed from the position of the center of gravity. The authors came to a conclusion similar to that of Murthy and Aharoni. Moreover, they determined the width at half-maximum of the MAXS lines to determine a measure for "order correlation length along meridional direction".

Our MAXS peaks originate from an electron density difference between smectic mesogenic layers and layers containing the spacer units of the LC polymer. To such an extent, they are closely related to the field of polymer nanostructure analysis, in which the structure of semicrystalline polymers is studied first with SAXS and then with established methods of data analysis, such as the correlation function method or interface distribution analysis.[16–20] Nevertheless, MAXS data analysis cannot be carried out with these established methods because they are based on the implication of stacks built from flat and extended layers of alternating electron density. Our experience with MAXS data shows that at least the implication of flatness appears to be seriously violated for the LC states of the polymers studied.

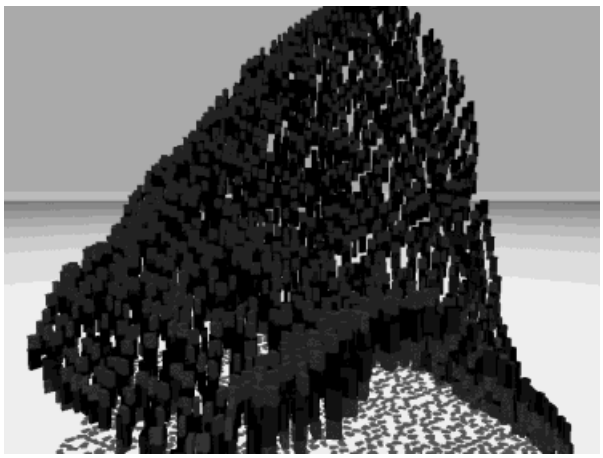

Figure 1. Sketch of a single layer of mesogens warped in physical space with a low degree of flatness. Imagine the next mesogenic layer following the visible contour in space almost perfectly.

THEORETICAL

Basic Notion

If a layer-line reflection is observed in fiber patterns, the lateral correlation among mesogens from the same layer is short-range only. Nevertheless, this does not imply that the layers have a limited lateral extension only. To model the observed scattering patterns, it is sufficient to assume that each of the layers is warped in space (cf. Fig. 1), whereas the directors of all mesogens remain pointing in the fiber direction and adjacent layers follow almost the same warp contour in space. In this notion, the observation of a layer line indicates a random warp of the layers in the

stack, whereas the gradual transition into a four-point pattern (indented layer line) would indicate lateral correlations beginning among undulations of the layers that, finally, might turn into a well-defined staggered arrangement of the mesogens in the layers. In this study, we are not trying to model such ordered structures but are aiming to describe layer structures that are strongly or moderately disordered.

Modeling the Layer-Line Reflection

For flat and extended layers, the lateral correlation function is unity because all the mesogens of each layer are perfectly aligned in a plane. Bearing in mind this ideal notion and real scattering patterns of, for example, semicrystalline polymers, one would resort to methods for line-profile analysis established in the field of small-angle scattering[18,21–23] and first shape the infinite stack (multiplication by a cylindrical-shape function) into a finite scattering entity. After introducing paracrystalline lattice distortions, averaging the statistics of an ensemble of such entities, and performing the solid angle average, one obtains an equation for the integral widths of the lattice reflections in which two sets (axial and lateral) of size and distortion parameters are contained. To separate the contributions, at least three orders of the long-period reflection must be analyzed. Thus, the classical method is well adapted to the medium-range order observed in semicrystalline polymers.

However, if among neighboring mesogens small random shifts with respect to the fiber direction are allowed, the loss of lateral correlation along the smectic layer may be considerable. Because of the assumed statistical nature, a gradual loss of correlation in the lateral direction may be described by a Gaussian, and in space a product of normalized Gaussians, separated in cylindrical coordinates (x_{12}, x_3), may serve as a first-order approximation to model a correlation body. This body is not an absolute scattering entity as defined in the classical approach. There is no visible domain boundary. Instead, the correlation body only defines a relative correlation range with respect to any deliberate monomer unit in the polymer material. Nevertheless, because of the strictly alternating mesogen-spacer structure and well-defined chain director, there are MAXS reflections. Then, resulting from the notion of a gradual correlation loss, the shape of such a reflection simply becomes

$$|\Phi|^2(s_{12}, s_3) = \exp(-4\pi^2\sigma_e^2 s_{12}^2)\exp(-4\pi^2\sigma_m^2 s_3^2) \tag{1}$$

with $s_{12} = (s_1^2 + s_2^2)^{1/2}$ and $s = (s_1^2 + s_2^2 + s_3^2)^{1/2} = (2/\lambda)\sin\theta$ being the magnitude of the scattering vector, where θ is half of the scattering angle. σ_e^2 and σ_m^2 are the variances of the Gaussians in physical space forming the correlation body in the equatorial and meridional directions, respectively. We identify σ_e as a measure of the flatness radius r_f and define

$$r_f = \sqrt{2}\sigma_e \tag{2}$$

because a circular disk of radius r_f is equivalent to the 2D integral width of the chosen 2D-Gaussian modeling the correlation body in the x_{12} plane. In a similar manner, we identify σ_m as a measure of the height h_s of the smectic lattice and define

$$h_s = \sqrt{2\pi}\sigma_m \tag{3}$$

Thus, any mesogen is surrounded by an imagined cylinder of radius r_f and height h_s, inside of which correlation is high and outside of which correlation is regarded as low. Without a loss of generality, let us treat a meridional layer line placed at ($\bar{s}_{12} = 0$, $\bar{s}_3 = 1$). Thus, we consider a reflection originating from a stack of layers with a long period equal to unity and s_3 defining the principal axis normal to the layers within the stack. Generalization to match a deliberate long period can easily be performed by appropriate scaling of space. Then, with eq 1 the scattering intensity, $I(\vec{s})$, becomes

$$I(\vec{s}) = \exp(-4\pi^2\sigma_e^2 s_{12}^2)\exp[-4\pi^2\sigma_m^2(s_3 - 1)^2] \tag{4}$$

The isotropical average intensity $I(s) = \langle I(\vec{s})\rangle_\omega$ of the corresponding powder pattern is computed from any pattern with fiber symmetry by

$$I(s) = \frac{1}{2}\int_0^\pi I(s, \psi)\sin\psi d\psi \tag{5}$$

with $\tan\psi = s_{12}/s_3$. For any result of practical interest,

$$\beta^2 = \sigma_m^2 - \sigma_e^2 > 0 \tag{6}$$

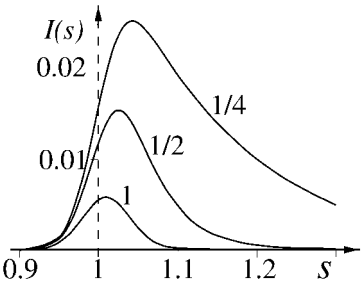

Figure 2. When the lateral correlation within smectic layers decreases, the MAXS line corresponding to the layer repeat in the chain direction shifts, broadens, and becomes more and more asymmetrical. Computation is based on eq 7 with the parameter $\sigma_m = 4$ and values of σ_e as indicated in the legend to the curves.

must be fulfilled because otherwise the reflection in the fiber pattern does not look like a layer line. Introduction of the variable β serves to simplify the result

$$I(s) = \frac{1}{8\sqrt{\pi}\,\beta s}\exp\left\{\left(\frac{2\pi}{\beta}\right)^2(\sigma_m^2 - \beta^2 s^2)(\sigma_m^2 - \beta^2)\right\} \times \left[\operatorname{erf}\left\{\frac{2\pi}{\beta}(\sigma_m^2 + \beta^2 s)\right\} - \operatorname{erf}\left\{\frac{2\pi}{\beta}(\sigma_m^2 - \beta^2 s)\right\}\right] \quad (7)$$

of the integration. In every case of practical interest, the observed MAXS reflection of the layer repeat is relatively narrow (i.e., σ_m and β are large) and positioned close to $s = 1$. Thus, we may simplify

$$\operatorname{erf}\left\{\frac{2\pi}{\beta}(\sigma_m^2 + \beta^2 s)\right\} = 1,$$

and

$$I(s) = \frac{1}{8\sqrt{\pi}\,\beta s}\exp\left\{\left(\frac{2\pi}{\beta}\right)^2(\sigma_m^2 - \beta^2 s^2)(\sigma_m^2 - \beta^2)\right\} \times \operatorname{erfc}\left\{\frac{2\pi}{\beta}(\sigma_m^2 - \beta^2 s)\right\} \quad (8)$$

is valid in excellent approximation. The results yield various shapes of MAXS lines, which for three sets of parameters are presented in Figure 2. The three curves describe layer stacks made from $h_s = 10$ correlated layers in the chain direction. From the drawing, we deduce that as soon as the range of flatness r_f decreases to values shorter than the lattice repeat in the chain direction (long period), the observed MAXS powder line becomes considerably shifted and asymmetric.

Indented Layer Lines

In the preceding section, we used a lens-shaped function as a model for the layer line and carried out the isotropization. In our experiments, we often observe indented layer lines. Therefore, it is necessary to find out how such layer lines transform when solid angle averaging is applied. To model indented layer lines, let us now choose two lenses of identical thickness σ_m in the meridional direction but of different diameter σ_e in the equatorial direction. We characterize these lenses from reciprocal space by variances in real space. Thus, if $\sigma_{ei} > \sigma_{eo}$, the lens with the parameter σ_{ei} (inner lens) is less extended than the one with the parameter σ_{eo} (outer lens). Subtracting these two lenses from each other, we end up with the representation of an indented layer line. With respect to Figure 2, the solutions

$$I(s) = \frac{1}{8\sqrt{\pi}\,\beta_o s}\exp\left\{\left(\frac{2\pi}{\beta_o}\right)^2(\sigma_m^2 - \beta_o^2 s^2) \times (\sigma_m^2 - \beta_o^2)\right\}\operatorname{erfc}\left\{\frac{2\pi}{\beta_o}(\sigma_m^2 - \beta_o^2 s)\right\} - \frac{D}{8\sqrt{\pi}\,\beta_i s}\exp\left\{\left(\frac{2\pi}{\beta_i}\right)^2(\sigma_m^2 - \beta_i^2 s^2) \times (\sigma_m^2 - \beta_i^2)\right\}\operatorname{erfc}\left\{\frac{2\pi}{\beta_i}(\sigma_m^2 - \beta_i^2 s)\right\} \quad (9)$$

are represented by differences between pairs of curves. In eq 9, the parameters $\beta_i^2 = \sigma_m^2 - \sigma_{ei}^2$ and $\beta_o^2 = \sigma_m^2 - \sigma_{eo}^2$ contain the different equatorial extensions of the basic functions, and the factor $0 \le D \le 1$ controls the amount of layer-line indentation.

As shown in Figure 3, even considerable indentations of the original layer line hardly change the shape and position of the MAXS line observed from the corresponding isotropic sample. We thus conclude that, to a first approximation, the position and asymmetric shape of a MAXS line from an isotropic smectic polymer material contain information predominantly on the correlation body of the smectic stack, that is, on the stack height h_s in the chain direction and on its range of flatness r_f at right angles to the chain direction. Structural information related to layer-line indentation or even splitting can hardly be extracted from the position and shape of the MAXS line. We admit that there is no physical meaning behind the operation of subtracting two line shapes in reciprocal space from each other, except for the fact that such a shape is a good fit to the observed

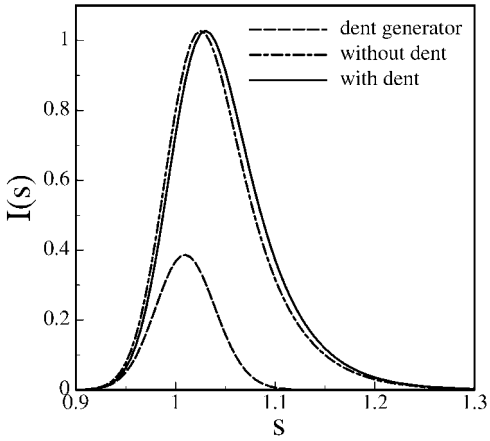

Figure 3. Solid-angle-averaged MAXS intensity of an indented layer line (solid line) according to eq 9 compared with the averaged intensity of an unindented layer line (dashed–dotted). For ease of comparison, the solid line has been multiplied by a factor of 1.19.

indented MAXS reflections and that it can easily be computed and spherically averaged.

RESULTS AND DISCUSSION

General Features of MAXS Data from a Heating Series

Figure 4 shows selected MAXS scattering curves collected during the continuous heating of an isotropic PEI material with synchrotron radiation. The initial material was prepared by quenching from the melt. The incident X-ray beam was pinhole-collimated. A narrow-beam cross section guaranteed negligibility of instrumental broadening. The wavelength of radiation was set to $\lambda = 0.15$ nm. Data presented were collected with 1D or 2D gas-filled detectors. The data were corrected for background scattering, sample absorption, and the decay of the primary intensity due to the decreasing intensity of the synchrotron beam. Because of the width of the observed broad peaks and the low scattering angle, intensity corrections for flat film geometry were considered unnecessary as far as the presented evaluation of data is concerned.

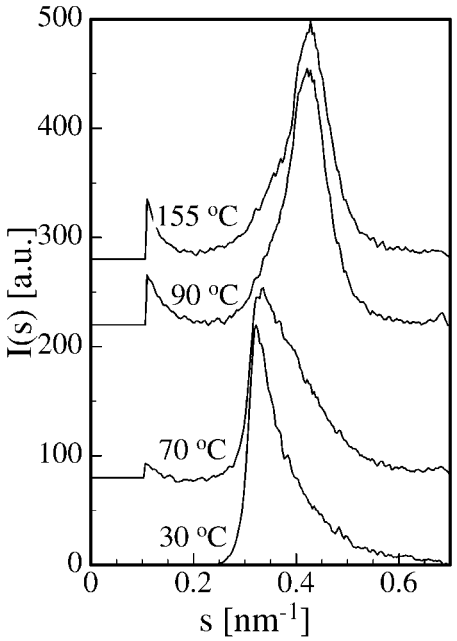

Figure 4. Selected MAXS scattering curves collected during the continuous heating of a quenched isotropic PEI sample.

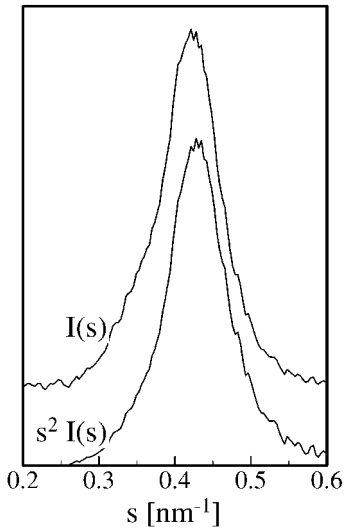

Figure 5. Isotropic MAXS $I(s)$ of the smectic crystalline phase (PEI at 90 °C) showing an asymmetric peak only before conversion into a linear scattering curve $[s^2I(s)]$.

All MAXS lines are broad and asymmetric. At low temperatures, the shape of the line, in principle, corresponds to the model curves presented in the Theoretical section. The steep gradient slope is on the left. Between 70 and 90 °C, position and shape undergo a transition that turns the slope with the steeper gradient to the right side of the curve. This finding is addressed as a transition from a frozen smectic LC phase to a smectic crystalline phase with stacks of extended smectic planes. If this is assessment is true, a multiplication of the curve by s^2 (cf. Fig. 5) yields a 1D scattering function that corresponds to the electron density distribution along the direction normal to the smectic planes. To verify that the asymmetric MAXS peak results from an (indent-

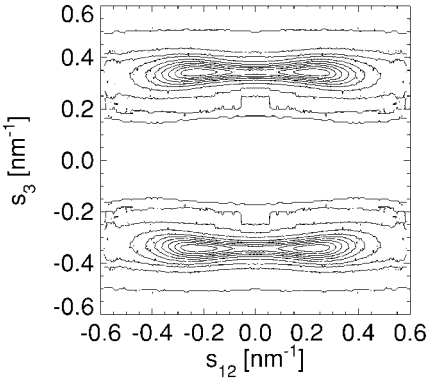

Figure 6. 2D MAXS pattern at 70 °C collected during the continuous heating of a PEI fiber drawn from the melt.

ed) layer-line pattern, fibers were drawn from the PEI melt and studied[24] during the same thermal treatment used for the isotropic material with a 2D detector. Figure 6 shows one of these images. All other patterns from the smectic LC phase are similar. A strong equatorial streak was not observed in the images from the oriented material. Faint streaks cannot be excluded but cannot be detected in the data accumulated with the setup used for technical reasons.

Quantitative Results Evaluated from MAXS Powder Diagrams

Figures 7 and 8 show measured MAXS peaks and fits according to eq 8 with the simplex algorithm

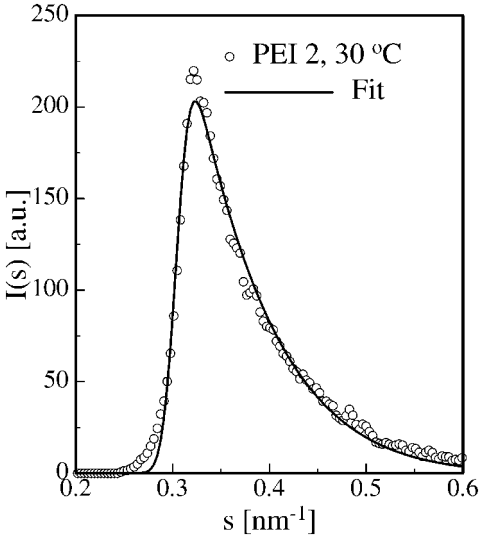

Figure 7. Fit of the isotropic MAXS peak from the smectic LC phase of PEI at 70 °C with the model according to eq 8.

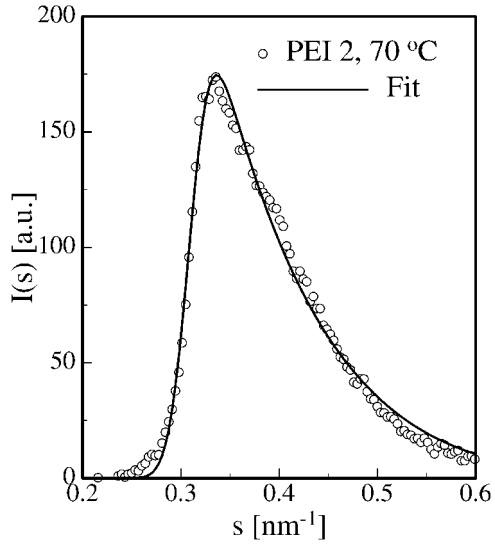

Figure 8. Fit of the isotropic MAXS peak from the smectic LC phase of PEI at 70 °C with the model according to eq 8.

for nonlinear regression. One observes that the model fits the curve sufficiently well. The structural parameters of the fits are presented in Table I. Intervals of confidence are computed from the parameter correlation matrix of the fit. The results in the table show that the relative range of flatness $r_f/L = \sqrt{2}\ \sigma_e/L \cong 0.25$ of the smectic layer is only one-quarter of the long period and does not change considerably between 30 and 70 °C. However, the number of well-correlated layers in the stack, $h_f/L = \sqrt{2\pi}\ \sigma_m/L$ decreases from 7.5 to 5 layers per stack. This finding is in good agreement with the corresponding values extracted from the fiber diagrams.

Comparison of Methods for the Determination of Smectic Layer Distances

Different methods for the determination of the distance between two adjacent smectic layers

Table I. Structural Parameters of the Best Fit of the Model in eq 8 to Two MAXS Curves from Isotropic PEI Material at Different Temperatures[a]

	30 °C	70 °C
W	1.87 ± 0.06	1.13 ± 0.03
L [nm]	3.28 ± 0.01	3.22 ± 0.01
σ_m/L	3.00 ± 0.11	2.08 ± 0.06
σ_e/L	0.18 ± 0.01	0.15 ± 0.01

[a] W is a scaling parameter, L is the long period in the meridional direction, and σ_m/L and σ_e/L are the widths of the correlation body with respect to the repeat unit of the smectic layer stacking.

Table II. Smectic Layer Distance Determined by Different Methods from the MAXS Line of a PEI Sample at Two Temperatures[a]

T (°C)	L_c (nm)	L_m (nm)	L_f (nm)
30	2.8	3.1	3.28 ± 0.01
70	2.7	3.0	3.22 ± 0.01

[a] L_c is determined from the center of the line, L_m is determined from the peak maximum position, and L_f is determined from the model fit (cf. Table I).

from the MAXS line are in use. Values determined on the same two data sets by three different methods are collected in Table II. As observed, the determination from the center of gravity results in values that are too low by more than 10%, whereas the determination from the peak maximum is quite close to the correct values.

CONCLUSIONS

If one observes layer-line reflections in MAXS from fibers of LC polymer materials or if MAXS lines corresponding to isotropic materials with a smectic structure show considerable anisotropy, one has to give up the notion of flat smectic layers (planes). If, nevertheless, one computes the layer repeat (long period) from the intensity maximum or, even worse, from the line's center of gravity, the computed value is systematically too low. If such an erroneously determined layer distance is compared to the sum of the lengths of mesogens and spacers, which may be computable from the known chemical structure, one might be misled. The scattering experiment shows that the smectic LC polymer is not a material with planar layers but instead is a material with lateral short-range order. The finite flatness of its layers can be determined from the asymmetry of the MAXS line with little error.

MAXS investigations were supported by HASYLAB Hamburg.

REFERENCES AND NOTES

1. Kricheldorf, H. R.; Probst, N.; Wutz, C. Macromolecules 1995, 28, 7990–7995.
2. Kricheldorf, H. R.; Probst, N.; Schwarz, G.; Wutz, C. Macromolecules 1996, 29, 4234–4240.
3. Blackwell, J.; Gutierrez, G. A.; Chivers, R. A.; Ruland, W. J Polym Sci Polym Phys Ed 1984, 22, 1343–1347.
4. Blackwell, J.; Gutierrez, G. A.; Chivers, R. A. Macromolecules 1984, 17, 1219–1224.
5. Blackwell, J.; Biswas, A.; Bonart, R. C. Macromolecules 1985, 18, 2126–2130.
6. Biswas, A.; Blackwell, J. Macromolecules 1987, 20, 2997–3002.
7. Biswas, A.; Blackwell, J. Macromolecules 1988, 21, 3158–3164.
8. Windle, A. H.; Viney, C.; Golombok, R.; Donald, A. M.; Mitchell, G. R. Faraday Discuss Chem Soc 1985, 79, 55–72.
9. Hanna, S.; Windle, A. H. Polymer 1988, 29, 207–223.
10. Hanna, S.; Lemmon, J.; Spontak, R. J.; Windle, A. H. Polymer 1992, 33, 3–10.
11. Mitchell, G. R.; Windle, A. H. Colloid Polym Sci 1985, 263, 230–244.
12. Mensinger, H.; Biswas, A.; Poths, H. Macromolecules 1992, 25, 3156–3163.
13. Francescangeli, O.; Yang, B.; Laus, M.; Angeloni, A. S.; Galli, G.; Chiellini, E. J Polym Sci Part B: Polym Phys 1995, 33, 699–705.
14. Murthy, N. S.; Aharoni, S. M. Macromolecules 1992, 25, 1177–1183.
15. Pardey, R.; Shen, D.; Gabori, P. A.; Harris, F. W.; Cheng, S. Z. D.; Adduci, J.; Facinelli, J. V.; Lenz, R. W. Macromolecules 1993, 26, 3687–3697.
16. Vonk, C. G.; Kortleve, G. Kolloid Z Z Polym 1967, 220, 19–24.
17. Vonk, C. G. J Appl Crystallogr 1978, 11, 541–546.
18. Strobl, G. R.; Müller, N. J Polym Sci Polym Phys Ed 1973, 11, 1219–1233.
19. Ruland, W. Colloid Polym Sci 1977, 255, 417–427.
20. Stribeck, N.; Ruland, W. J Appl Crystallogr 1978, 11, 535–539.
21. Crist, B.; Morosoff, N. J Polym Sci Polym Phys Ed 1973, 11, 1023–1045.
22. Crist, B. J Polym Sci Polym Phys Ed 1973, 11, 635–661.
23. Matyi, R. J.; Crist, B, Jr. J Polym Sci Polym Phys Ed 1978, 16, 1329–1354.
24. Wutz, C. Mol Cryst Liq 1997, 307, 175–188.